AIAA/AAS Astrodynamics Specialist Conference **AIAA-2010-8375**
August 2-5, 2010, Toronto, Canada

Analysis and Design of Fictive Post-2029 Apophis Intercept Mission for Nuclear Disruption

Sam Wagner* and Bong Wie †
Asteroid Deflection Research Center-Iowa State University, Ames, IA, USA

An impact from asteroid 99942 Apophis now seems unlikely (with an impact probability of approximately four-in-a million). However, in this paper it will be assumed that Apophis passes through a keyhole in 2029 and is inserted into a resonant orbit that will result in an impact on April 13th, 2036. Launch dates utilizing an Interplanetary Ballistic Missile system, capable of carrying up to a 1500 kg nuclear payload, and a total ΔV of 4 km/s are determined. Mission analysis for the 0-revolution rendezvous and intercept mission is performed as well as multiple revolution missions and more complicated mission designs which allow for rendezvous missions to be launched after the last feasible short 0-revolution rendezvous case. In this study it is assumed that for a subsurface nuclear explosion Apophis must be intercepted at least 15 days prior to Earth impact on April 13th, 2036. It is also assumed that if Apophis passes through the keyhole in 2029 a high energy nuclear deflection mission will be required to ensure Apophis doesn't impact the Earth.

Nomenclature

a	Semi-major Axis (AU or km)
AU	Astronomical Unit
C_3	Earth Escape Energy km^2/s^2
e	Eccentricity
GTO	Geostationary Transfer Orbit
H	Absolute Magnitude
i	Inclination (deg)
I_{sp}	Specific Impulse (s)
ISV	Integrated Space Vehicle
IPBM	Interplanetary Ballistic Missile
kT	Kiloton
LV	Launch Vehicle
LEO	Low Earth Orbit
m	Mass (kg)
M	Mean Anomaly Angle (deg)
mT	Megaton
NASA	National Aeronautics and Space Administration
NED	Nuclear Explosive Device
NEO	Near-Earth Object
OTV	Orbital Transfer Vehicle
TMV	Terminal Maneuvering Vehicle
ΔV	Change in Velocity (km/s)
θ	True Anomaly (deg)
Ω	Right Ascension of Ascending Node (deg)
ω	Argument of Periapsis (deg)

*Graduate Research Assistant, Dept. of Aerospace Engineering, 2271 Howe Hall, AIAA Student Member.
†Vance Coffman Endowed Chair Professor, Dept. of Aerospace Engineering, 2271 Howe Hall, AIAA Associate Fellow.

I. Introduction

Asteroids and comets have collided with the Earth in the past and will do so in the future. Throughout Earth's history these collisions have had a significant role in shaping Earth's biological and geological histories. For example, the extinction of the dinosaurs is widely believed to have been caused by the collision of an asteroid or comet. In the recent past, near-Earth objects (NEOs) have collided with the Earth, most notably the Tunguska event which occurred in Siberia in 1908. The impact is estimated to have released an explosion on the order of 3-5 megatons of TNT. The Tunguska incident was relatively harmless given the sparse population of Siberia. However, if an impact of this relatively low magnitude were to occur in a highly populated area the result would be devastating. For the first time in human history we have the technical knowledge and capability to launch a deflection mission to help ensure the survival of the human race.

This paper will focus on the mission analysis and design to asteroid 99942 Apophis, assuming it passes through the keyhole during the April 13th, 2029 close encounter with the Earth. However, it is assumed that a deflection mission decision will be made after confirming the 2029 keyhole passage. The methods presented in this paper can be used to design a mission to any asteroid or planetary body. The Apophis mission presented in this paper is merely a demonstration of the capabilities of the mission analysis software developed in house at the Asteroid Deflection Research Center (ADRC). Throughout the paper possible trajectories and launch windows for a deflection mission, both rendezvous and direct intercept missions, to Apophis will be determined. The orbital elements of the hypothetical perturbed orbit and physical parameters for Apophis are given in Tables 1(a) and 1(b) respectively.

Table 1: Orbital and physical parameters used for the hypothetical Apophis orbit. [1]

(a) Orbital elements

Elements	Value
epoch MJD	64699
a, AU	1.108243
e	0.190763
i, deg	2.166
Ω, deg	70.23
ω, deg	203.523
M_0, deg	227.857

(b) Physical parameters

Physical Parameter	Value
Rotational Period (hr)	30.5
Mass (kg)	2.1E+10
Diameter (m)	270
H	19.7
Albedo	0.33

A recent study has concluded that it may be feasible to significantly reduce the impact damage from an Earth-impacting NEO using a nuclear subsurface explosion as late as 15 days prior to impact. [2] The subsurface explosion is used to fragment the asteroid in such a way that a very small percentage of the asteroid impacts the Earth. This method is viable only for relatively small NEOs with diameters of at most a few hundred meters. This method would require a much longer mission lead time for asteroids with diameters in the kilometer range. A mitigation mission within a few weeks of impact requires a nuclear subsurface explosion due to large energy required to fragment the asteroid and ensure the majority of the resulting fragments disperse sufficiently to miss the Earth. Most proposed asteroid deflection methods, such as a kinetic impactor or gravity tractor, require large lead times to impart a ΔV significant enough to ensure the asteroid misses the Earth. [3] For this reason the previously proposed kinetic impactor or gravity tractor are not appropriate after Apophis passes through the keyhole in 2029 and is already in a resonant orbit that results in an future impact.

For this study the Interplanetary Ballistic Missile (IPBM) system architecture, previously proposed by the ADRC, [4] would be used to deliver the nuclear payload to Apophis. This proposed system consists of a launch vehicle (LV) and an integrated space vehicle (ISV). The ISV consists of an orbital transfer vehicle (OTV) and a terminal maneuvering vehicle (TMV) which is responsible for housing the nuclear payload(s). For this study the Delta IV Heavy launch vehicle configuration has been chosen as the launch vehicle for the primary IPBM system. This configuration is capable of delivering a 1500-kg NED and is capable of ΔVs of 3.5-4.5 km/s, depending on the specific final configuration chosen. The primary IPBM system departs from a geostationary transfer orbit (GTO) in order to minimize the ΔV required by the ISV. A secondary IPBM system employs a Delta II class LV (includes Taurus II) with a smaller ISV that delivers a 500-kg NED. In this case the IPBM would be injected directly into an Earth-escape orbit and then supplemented by the onboard propulsion system when necessary. The primary Delta IV Heavy configuration can deliver up to a 1.5-mT nuclear payload, while the secondary system can deliver a 500-kT nuclear payload. A kiloton (kT) of

TNT is equal to an energy of $4.18\text{x}10^{12}$ Joules.

It will be shown that for the hypothetical post-2029 Apophis mission, that the primary IPBM system is capable of both rendezvous and intercept missions. Several launch dates during the 7 year period from passing through the keyhole to Earth impact have been determined. Included in these launch windows is a "last minute" mission, capable of intercepting Apophis 1-2 months prior to impact. The focus of this paper is on the mission analysis and the development of the software needed to complete the analysis. It is assumed that the maximum ΔV limit used to determine launch windows is 4 km/s, corresponding to the primary IPBM system.

In addition to evaluating the mission requirements for a post 2029 mission to Apophis, which on a hypothetical collision course, the purpose of this paper is to outline the methods used to create a software package, primarily in in Matlab, capable of searching for trajectories and launch windows, requiring only the ephemeris data of the desired destination. Various ΔV plots and trajectories obtained using this software are provided in Appendix A. An outline of methods used for the Lambert solver can be found in Appendix B. This software currently includes the evaluation of both the interception and rendezvous missions, as well as the ability to search for crewed mission launch dates.[5] The intercept mission refers to a mission which doesn't require an arrival ΔV, while the rendezvous mission refers to a mission where an orbit is obtained in which the relative speed between Apophis and the ISV is essentially zero. The current version of the software has the ability to search for standard type 1 (less than 180°) and type 2 (180° to 360°) transfer trajectories, as well as the ability to search for multiple revolution mission. Future versions of the software will include the ability to search for single and multiple gravity assists, resonant orbits, and phasing orbits. This paper is essentially a case study to show the capabilities of the software that has been developed. This software has been validated by reproducing graphs and trajectories for a mission to Apophis for a radio tagging mission[6] as well other proposed missions.

II. Mission Analysis and Design

In this section both the rendezvous and intercept missions will be analyzed. Preliminary analysis of a single gravity assist at Venus or Mars didn't produce any trajectory with a total ΔV lower than the quick transfer (0-revolution and 1+ revolution) solutions discussed in the following sections. With a maximum notice of 7 years, missions with multiple gravity assists such as Galileo's Venus-Earth-Earth gravity assist would likely not allow for interception before the Earth-Apophis collision in 2036. Missions using multiple orbits prior to arrival have been found and shown in general to reduce the required total mission ΔV as well.

The mission design software was used to determine the so-called porkchop plot, a plot of minimum ΔV, for each launch date range, and optimal trajectories for each launch window. For the rendezvous mission analysis, the maximum mission length allowed for the search was 1000 days for the 0-revolution and 2000 days for the multiple revolution solutions. In most cases the minimum ΔV missions were found within the first thousand days of departure, but more were included to ensure the minimum ΔV mission wasn't skipped on during the search. The maximum mission length for the intercept mission used in this study is also 1000 days. This allows for an interception mission to be carried out at almost anytime during the 7 year period searched. As previously mentioned a departure from a geostationary transfer orbit, as considered for the IPBM system, is assumed during the following analysis.

A. 0-Revolution Rendezvous Mission Analysis

A contour plot of the total ΔV for the time-of-flight (the number of days to rendezvous) versus launch dates is shown in Figure 1. This kind of contour plot is often called the porkchop plot. Careful analysis of this porkchop plot indicates that launch windows will be available from 2029 into the early 2030's. Although hard to see, there is one short 5 day launch windows in 2035 as well. The main constraint for launch windows after 2035 is that interception must occur at least 15 days prior to the Earth-Apophis collision.[2] For this reason all figures and tables in this paper represent only missions which arrive at least 15 days prior to impact.

Launch windows can be determined by examining Figure 2, which is a plot of minimum total ΔV versus launch date from 2029 to 2036. To determine the launch windows a maximum ΔV of 4 km/s was used, corresponding to the chosen IPBM configuration. There are 4 possible launch windows from 2029 to 2031 and a short 5 day launch window in April of 2035. Between 2031 and 2035 and afer the 2035 launch window there are no possible rendezvous launch windows prior to impact in 2036. Information for the nominal departure date for each windows can be found in Table 2. This table shows the magnitudes and dates for the Earth departure and Apophis arrival burns as well as the starting and ending dates for each corresponding launch window.

Each separate launch window plot is shown in Appendix A. For each launch window plot, the Earth departure,

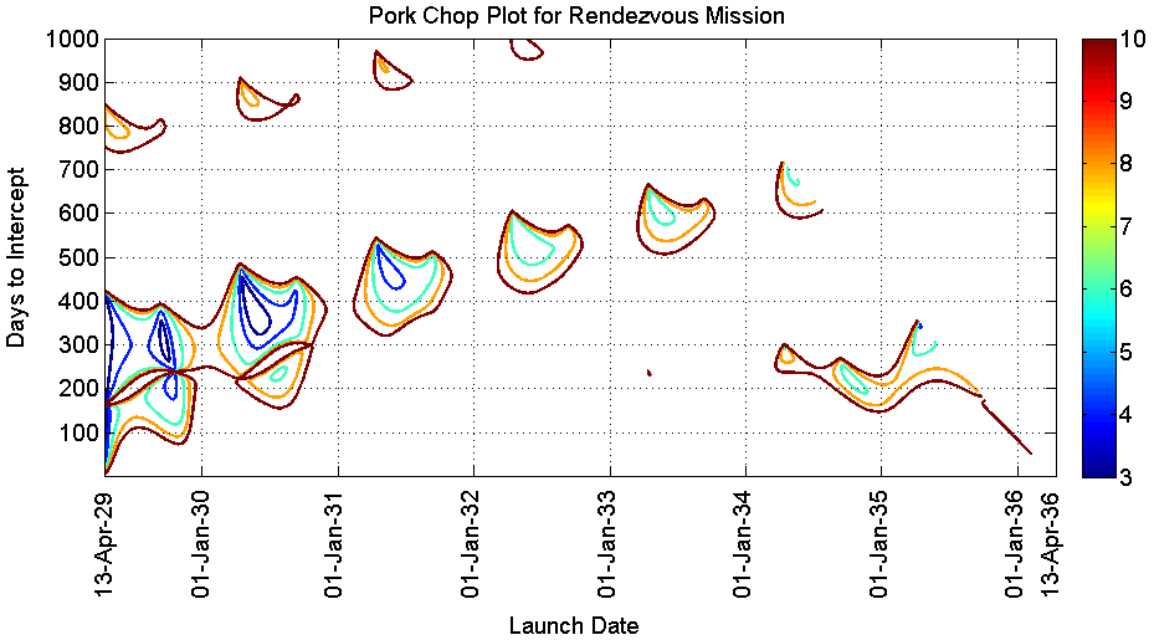

Figure 1: Total ΔV porkchop plot of the time-of-flight versus launch date for the rendezvous mission.

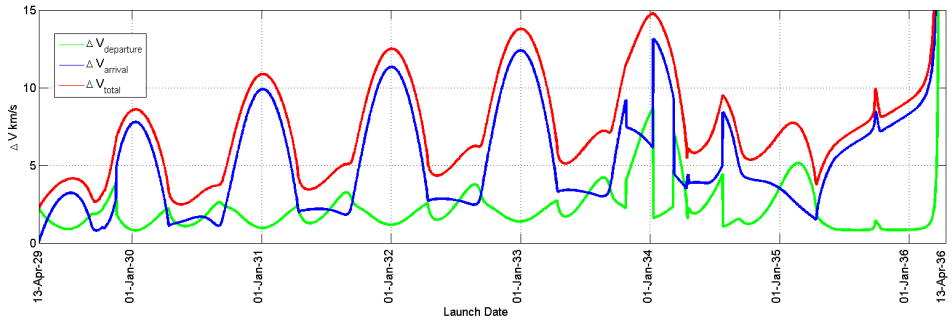

Figure 2: Minimum total ΔV versus launch date from 4/13/2029 to 4/13/2036.

Apophis arrival and total ΔV's are provided. Launch windows range anywhere from 70-155 days in length, with the exception of launch window 5. If desired this is enough time to launch multiple IPBM's in order to increase the probability of a successful mission. Analysis of these launch windows shows significant variations in the Earth departure (1-2.2 km/s) and Apophis arrival (0.1-2.15 km/s) maneuvers.

The arrival dates corresponding to the early launch windows are shown in Figure 3. With the exception of the short 5 day window in 2035 it is not possible to launch a rendezvous mision after 2031. It is likely that a decision to launch a deflection mission would not be made prior to mid-2031, thus other possible mission designs must be found. For this reason "last minute" disruption and multiple revolution rendezvous missions will be discussed as well in this paper.

The transfer trajectory corresponding the first launch window is shown in Figure 4. The trajectories for the other 4 launch windows can be found in Appendix A. It can be seen from each of the trajectory plots that the typical Sun-Apophis approach angles are in the 90° range. Further analysis of the Sun-Apophis approach or phase angles may be needed for future terminal-phase guidance analysis and design.

B. 0-Revolution Direct Intercept Mission

After April of 2035 there are no feasible rendezvous launch windows, which means that a direct intercept mission would be required for any "last minute" deflection missions. It is likely that developing and building a spacecraft such as the proposed IPBM system would take several years. It also seems likely that development would not start until

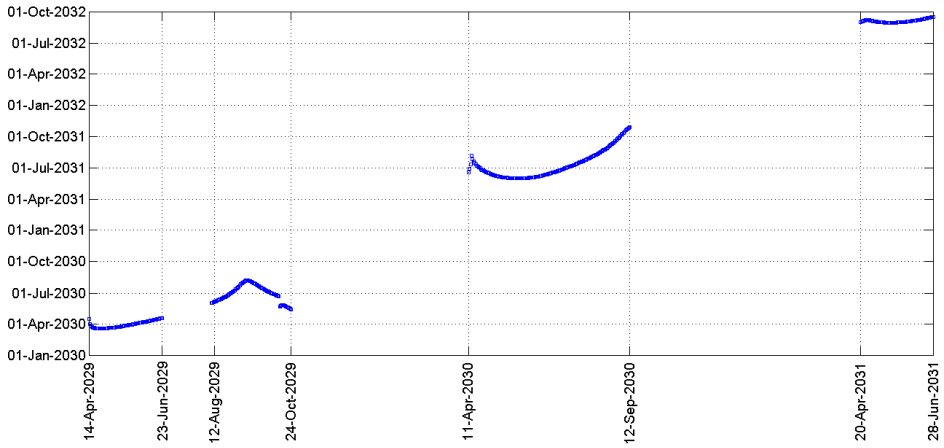

Figure 3: Arrival dates for the first four launch windows.

Table 2: Minimum ΔV transfer trajectory for each optimal 0-revolution launch date.

0-Revolution Launch Windows								
Mission Information	**Departure Date**	**Departure ΔV (km/s)**	**Arrival Date**	**Arrival ΔV (km/s)**	**Total ΔV**	**Window Start**	**Window End**	**Length (days)**
Window 1	13-Apr-29	2.186	16-Apr-30	0.102	**2.289**	13-Apr-29	23-Jun-29	**71**
Window 2	12-Sep-29	1.867	26-Jul-30	0.801	**2.668**	12-Aug-29	24-Oct-29	**73**
Window 3	20-May-30	1.091	2-Jun-31	1.460	**2.552**	11-Apr-30	12-Sep-30	**154**
Window 4	15-May-31	1.281	30-Aug-32	2.156	**3.436**	20-Apr-31	28-Jun-31	**69**
Window 5	15-Apr-35	2.045	28-Mar-36	1.702	**3.747**	13-Apr-35	18-Apr-35	**5**

after Apophis has passed through the keyhole in 2029, this is due to the four-in-a million chance this will happen. With the last low ΔV rendezvous 0-revolution launch window ending a little more than 2 years after the 2029 close encounter, it may be desirable to launch either a direct intercept or multiple revolution mission. For this reason a direct intercept and multiple revolution missions will be analyzed in the following sections. A total ΔV contour plot of the time-of-flight versus launch date is shown in Figure 5. From this plot it can be seen that an intercept mission with a maximum ΔV of 4 km/s is possible at almost continuously from 2029-2036.

Recent research[2] has shown that it may be possible to prevent all but a few percent of the material from an asteroid from impacting the Earth by utilizing a nuclear subsurface explosion. However, such a disruption mission requires a rendezvous with Apophis to provide an acceptable penetrator velocity of 300 m/s. However, it may also be possible to design a high speed penetrator. The objective of this section is to determine the feasibility of a last minute rendezvous mission launched anywhere from 2-3 years to as little as 20-30 days prior the the 2036 impact. This requires further analysis of Figure 5. An expanded version of Figure 5 showing only this time span is provided in Figure 6.

Careful analysis of Figure 6 shows that late launch dates ranging from 3/28/2035 to 3/19/2036 are feasible for the intercept mission. The last feasible launch date is 25 days prior to impact. Using the IPBM system architecture, it may be feasible to launch a last minute intercept mission to disrupt an NEO similar to Apophis. No limits on the arrival velocity have been imposed in Figures 5 and 6. Unfortunately, the penetrator's maximum impact velocity is currently limited by 300 m/s, which means the the late intercept mission concept may not be a viable option. In this situation either a nuclear surface explosion (contact burst) or high-speed penetrator (>5 km/sec impact velocity) must be developed and employed. An example of late intercept trajectory is shown in Figure 7, with all necessary mission data shown in Table 3.

To fully determine the feasibility of the late intercept mission, further information is needed on an intercept penetrator used for the nuclear subsurface explosion. In general, the later the intercept launch occurs the higher the arrival V_∞ at Apophis. Intercept launch dates in the 2034-2035 range generally have an intercept velocity (at Apophis) in the 5-6 km/s range.

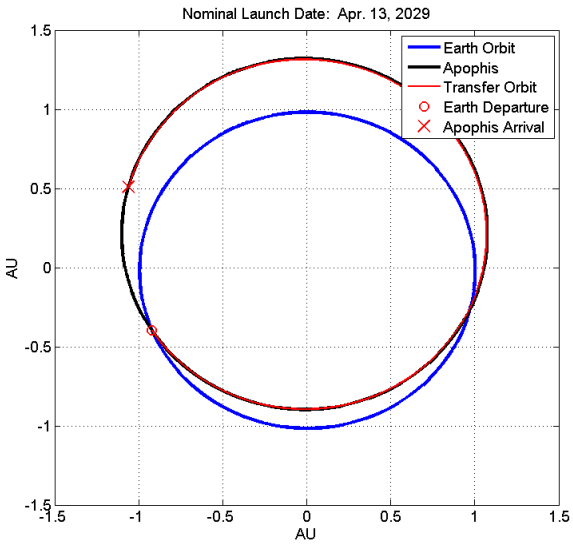

Figure 4: Nominal trajectory launch window 1. Trajectory shown in (X,Y) plane of J2000 coordinate system.

Table 3: Mission information for the example last minute intercept mission

Example Trajectory	
Departure Date	26-Feb-36
Arrival Date	19-Mar-36
Total ΔV, km/s	2.830
Semi-major axis, AU	1.714
Eccentricity	0.441
Inclination, deg	2.032
Ω, deg	336.944
ω, deg	153.860
Departure θ, deg	26.163
Arrival θ, deg	50.231

C. Multiple Revolution Mission Analysis

In this section results from a multiple revolution search will be presented. However, only the results from the search which allow one complete revolution will be presented. The results from the two and three revolution search was very similar to the one revolution case. In general the lengths of the early launch windows were significantly increased, but later launch windows were not possible due to high mission lengths required. The multiple revolution Lambert solution has been examined intensively by astrodynamics researchers throughout the past few decades.[7–11] Among the various approaches, the universal solution method for the multiple revolution Lambert problem, which seems to be an efficient and robust approach, is summarized in Appendix B.[11,12]

By performing a 1+ revolution search it is shown that in general mission ΔV's are lower when compared to the 0-revolution solutions discussed earlier. This allows for more launch dates in the 2032-2035 period that were not previously possible. When performing a multiple revolution search there are always two solutions found for each Lambert solution. The two solutions consist of a solution with a smaller semi-major axis and a larger semi-major axis. For this reason the two solutions will be referred to as the low-energy and high-energy solutions respectively. No analysis of the multi-revolution direct intercept mission will be performed because of the nearly continuous 0-revolution direct intercept launch windows. Analysis of the multi-revolution direct intercept mission can be performed in the future if additional intercept velocity constraint are found in the future.

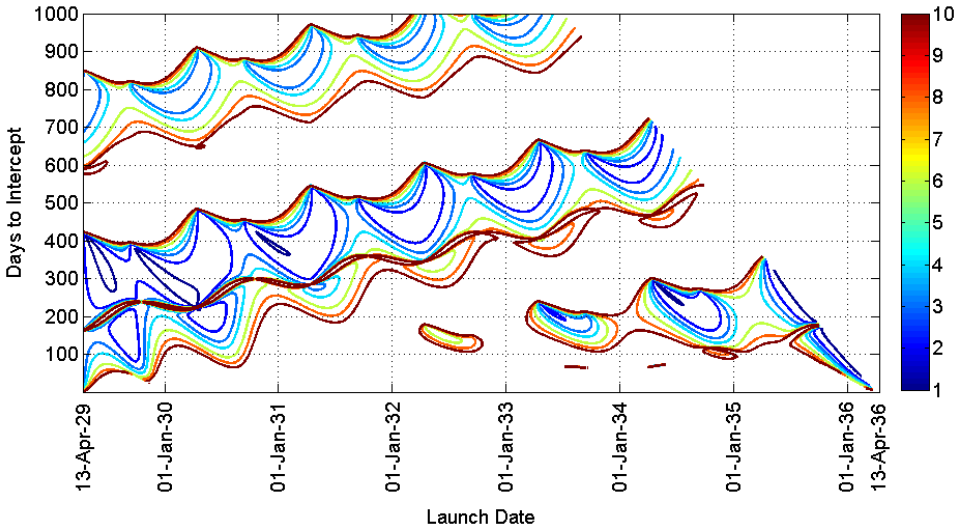

Figure 5: Porkchop plot for the direct intercept mission.

1. Low-Energy Rendezvous Mission Analysis

As the name suggests the low-energy solutions generally require a smaller ΔV than both of the corresponding 0-revolution and high-energy missions. Consequently, most of the additional launch dates determined by the multi-revolution (prior to Apophis arrival) search are part of the low-energy solutions. A porkchop plot of the number of days to Apophis interception versus launch date, similar to Figure 1, is shown in Figure 8. From this porkchop plot it can be determined that the optimal mission lengths occur in the 600-1000 days range, slowly increasing as the launch date increases. Several launch dates similar to the 0-revolution rendezvous mission exist prior to May of 2031. However, it can be easily seen from the porkchop plot that additional launch windows exist as well during other unaccessible period for the 0-revolution mission. These additional launch windows occur from April of 2031 to April of 2034, a period where rendezvous 0-revolution missions were not possible.

The 8 possible launch windows can be easily seen in Figure 9. This is a plot of the total ΔV as well as the Earth departure and Apophis arrival ΔV's. For all dates searched the last possible arrival date is March 29th, 2036, 15 days prior to impact. The intercept date limitation is the reason that no 1-revolution solutions exist after early 2035, particularly low ΔV solutions. Analysis of this plot shows that a total of 8 launch windows exist, with the last 5 windows opening up launch dates that were previously unavailable for the 0-revolution rendezvous mission. The accompanying window ranges and information for the nominal departure date for launch window are shown in Table 4. In general the launch window lengths are similar, perhaps slightly longer for the 1-revolution case when compared to the 0-revolution windows. However, when performing a 2-3 revolution search, the early launch windows are drastically lengthened when compared to the 0-revolution case. No additional launch windows were found for 2+ revolution case, so no further analysis will be presented.

Figure 10 shows the arrival dates for each launch date in the 8 launch windows found. It can be easily seen that for launch windows 6 and 8 the spacecraft arrives on or just prior to March 29th, 2036 (15 days prior to impact). Analysis of Table 4 reveals that the minimum total ΔV required for these two launch windows is higher than all of the 6 other launch windows. This is caused by the time constraints imposed by this study. A comparison of Tables 2 and 4 reveals that in general the total ΔV is lower for the 1-revolution low-energy solution versus the 0-revolution rendezvous mission. This confirms the early statement that adding in multiple revolutions lowers the total ΔV requirements for similar launch windows.

An example trajectory for a 1-revolution rendezvous mission is shown in Figure 11. The particular trajectory shown is from the nominal launch date during launch window 4 in Table 4. Like the 0-revolution trajectories Apophis is generally approached from behind Apophis, with roughly a 90° sun angle. Earth departure usually occurs near either of the 2 points where the Earth crosses Apophis' orbit.

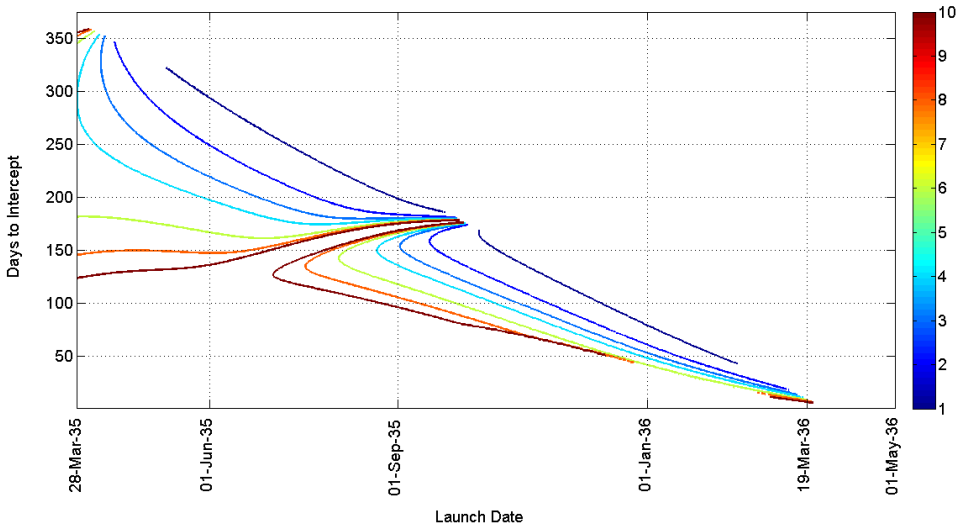

Figure 6: Total ΔV contour plot of the flight-of-time versus launch dates from 4/13/2029 to 4/13/2036 for the intercept mission.

Table 4: Minimum ΔV transfer trajectory for each optimal 1-revolution low-energy launch window.

1-Revolution Low-Energy Launch Windows								
Mission Information	**Departure Date**	**Departure ΔV (km/s)**	**Arrival Date**	**Arrival ΔV (km/s)**	**Total ΔV**	**Window Start**	**Window End**	**Length (days)**
Window 1	13-Apr-29	2.242	7-May-31	0.013	**2.255**	13-Apr-29	16-Jun-29	**64**
Window 2	24-Sep-29	2.053	25-Sep-31	0.7394	**2.793**	30-Jul-29	4-Oct-29	**66**
Window 3	10-May-30	1.324	29-Jun-32	0.8449	**2.169**	5-Apr-30	18-Sep-30	**166**
Window 4	20-May-31	1.123	3-Oct-33	1.3812	**2.505**	11-Apr-31	27-Aug-31	**138**
Window 5	16-May-32	1.194	22-Dec-34	1.7989	**2.992**	13-Apr-32	18-Jul-32	**96**
Window 6	13-May-33	1.293	2-Mar-36	2.1871	**3.480**	18-Apr-33	22-Jun-33	**65**
Window 7	28-Oct-33	0.905	4-May-35	2.5233	**3.429**	18-Sep-33	17-Dec-33	**90**
Window 8	15-Apr-34	2.008	28-Mar-36	1.7413	**3.750**	12-Apr-34	18-Apr-34	**6**

2. *High-Energy Rendezvous Mission Analysis*

As the name would suggest the high-energy solutions generally require a higher ΔV than the low-energy solution, often very similar to that required by the 0-revolution rendezvous mission. For this reason the high-energy solutions yield launch windows very similar to the 0-revolution case. However the high-energy solution does open up a few launch dates that are unaccessible by the 0-revolution case.

The total ΔV plot versus launch date for this case is shown in Figure 12. When compared to the low-energy solution the total ΔV for the high-energy is in most cases significantly higher, resulting in few launch windows. The launch windows made possible with the high-energy 1-revolution solution are very similar the the windows found for the 0-revolution case. The launch window information for the high-energy solution can be found in Table 5. Launch window 5 is the only high-energy launch window that opens up potential launch windows not feasible for the 0-revolution case. Other than a slight extension of launch dates the high-energy solutions offer very few advantages over the 0-revolution case. The only time these solutions would be useful is if a later arrival date than the 0-revolution case is desired.

Throughout this section multiple launch windows have been found for a rendezvous mission to Apophis. Launch windows close to the original Earth-Apophis close encounter and approximately 1 year prior to impact are possible using a traditional 0-revolution Lambert search. The latest 0-revolution rendezvous launch window is only 5 days long and requires a minimum ΔV of 3.747 km/s, potentially problematic if a launch error or delay were to occur during this

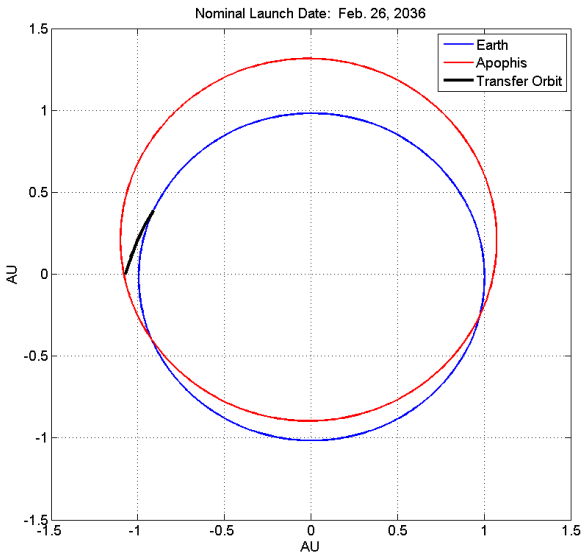

Figure 7: Trajectory for a late intercept mission. Trajectory shown in (X,Y)-plane of J2000 coordinate system.

Table 5: Minimum ΔV transfer trajectory for each optimal 1-revolution high-energy launch window.

1-Revolution High-Energy Launch Windows								
Mission Information	**Departure Date**	**Departure ΔV (km/s)**	**Arrival Date**	**Arrival ΔV (km/s)**	**Total ΔV**	**Window Start**	**Window End**	**Length (days)**
Window 1	13-Apr-29	2.215	13-Aug-30	0.088	**2.304**	13-Apr-29	13-May-29	**30**
Window 2	7-Sep-29	2.261	26-Nov-30	1.321	**3.581**	25-Aug-29	21-Sep-29	**27**
Window 3	29-Sep-29	2.730	13-Apr-31	0.913	**3.643**	25-Sep-29	1-Oct-29	**6**
Window 4	8-Aug-30	1.203	19-Mar-32	1.217	**2.420**	10-Apr-30	14-Sep-30	**157**
Window 5	6-Aug-31	1.197	30-Mar-33	2.123	**3.320**	22-Jun-31	3-Aug-31	**42**

short period. A minimum ΔV of 3.747 km/s is also very close to the 4 km/s maximum used for this study, allowing little room for error and course corrections. For this reason a 1-revolution launch window and trajectory search, both the high and low-energy solutions are presented, was performed. It has been shown that such a mission opens up approximately 5 new launch windows (there is some overlap in launch windows) during periods (2031-2035) when they are otherwise not feasible. Various trajectories and ΔV plots for the 0-revolution and 1-revolution case are shown in Appendix A.

For the direct intercept mission (non-rendezvous) only the 0-revolution case has been analyzed. This is because there are nearly continuous launch dates for this mission. The direct intercept mission has arrival speeds ranging from under 1 km/s to 20+ km/s, making it difficult to perform any additional analysis with more arrival velocity or direction constraints. This topic would be much more suited for a future study aimed at evaluating the terminal guidance logic and requirements for such an intercept mission.

Further information on the software used to complete the mission analysis and methods employed can be found in Appendix B. This includes the 0 and multiple revolution lambert solutions. Not all the Lambert solution methods tested are shown in Appendix B.

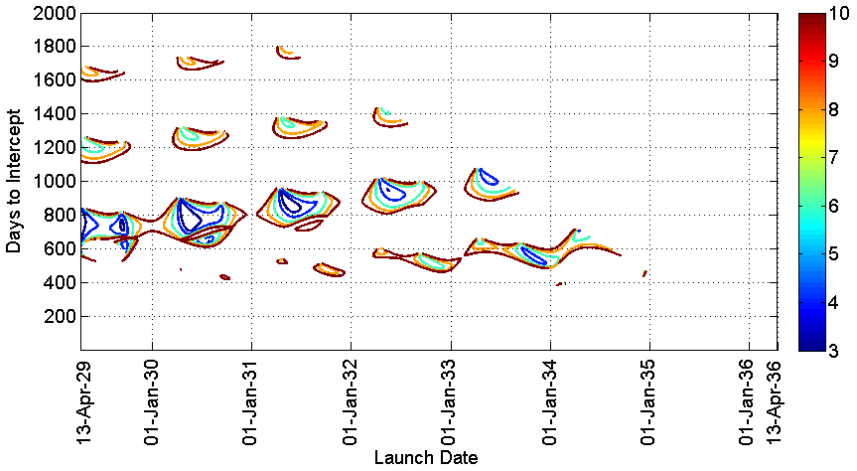

Figure 8: Total ΔV contour plot of the time-of-flight versus launch dates from 4/13/2029 to 4/13/2036 for the 1-revolution low-energy solution rendezvous mission.

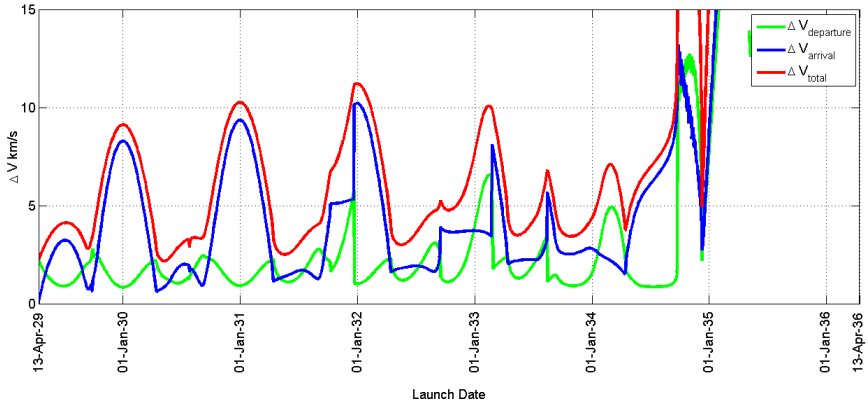

Figure 9: Minimum total ΔV versus launch date from 4/13/2029 to 4/13/2036 for the 1-revolution low-energy solutions.

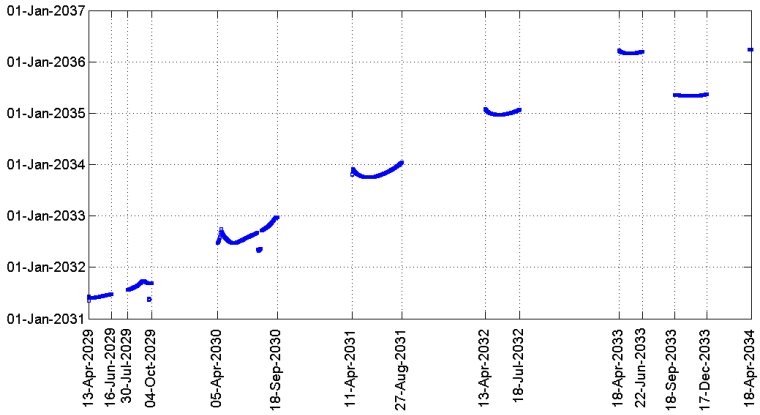

Figure 10: Arrival dates for the 8 launch windows for the 1-revolution low energy solutions.

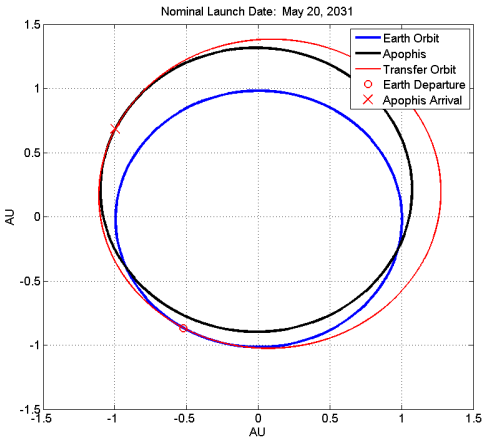

Figure 11: Nominal trajectory launch window 4 for the low-energy 1 revolution solution. Trajectory shown in (X,Y) plane of J2000 coordinate system.

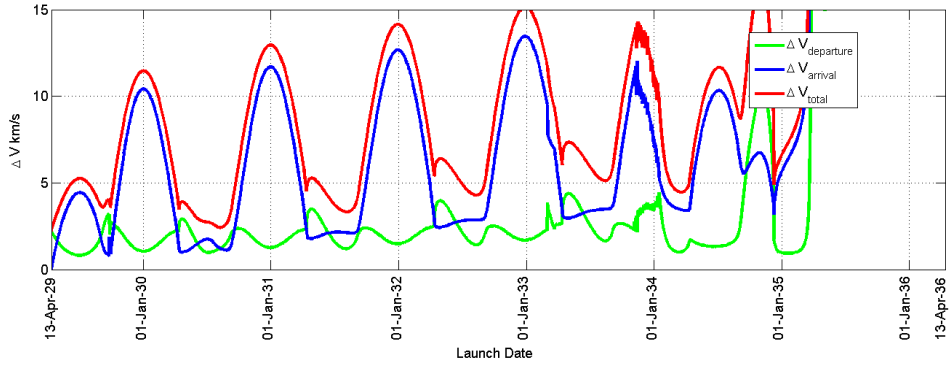

Figure 12: Minimum total ΔV versus launch date from 4/13/2029 to 4/13/2036 for the 1-revolution high-energy solutions.

III. Conclusion

With rendezvous launch windows occurring throughout the 7 year time span, a nuclear deflection mission utilizing a subsurface explosion is possible. The last rendezvous launch date is in April of 2035. It is highly unlikely that a system such as the IPBM will exist prior to the 2029 keyhole passage. This means that an IPBM or similar architecture will have to be developed and tested prior to April of 2035. Assuming this is true, missions utilizing the early launch dates found for the 0-revolution mission will also be not feasible. The later low-energy 1-revolution mission will likely be required for a nuclear penetrator mission.

Analysis of a fictive post-2029 Apophis mission has resulted in 18 possible launch windows/missions, with a some launch date overlaps. Launch windows for a rendezvous mission, required for a nuclear subsurface explosion, have been found from April 13th, 2029 up to April 18th, 2035. The direct intercept mission analysis has also been performed to determine the feasibility of late intercept missions. It has been shown that intercept missions, without arrival velocity constraints, are possible up to 25 days prior to impact. However, such a late launch may not be a viable option. Current nuclear subsurface penetrators are limited to an impact speed in the 300 m/s range, significantly lower than the typical arrival velocities found for the direct intercept mission. For this reason the late launch intercept mission will require a further tradeoff study of nuclear subsurface versus surface explosions.

Appendix A: Mission Plots and Trajectories

In this appendix mission ΔV plots and trajectories will be included for the zero and multiple revolution cases.

0-Revolution Nonimal Trajectories

Rendezvous Mission Plots

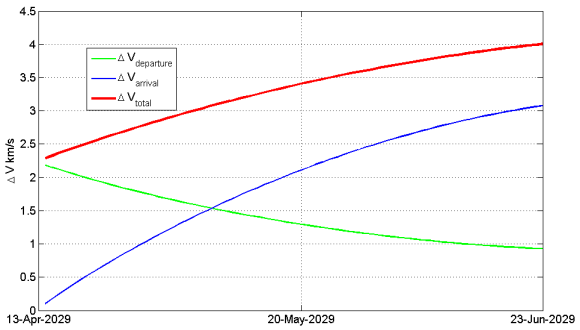

Figure 13: Launch window 1.

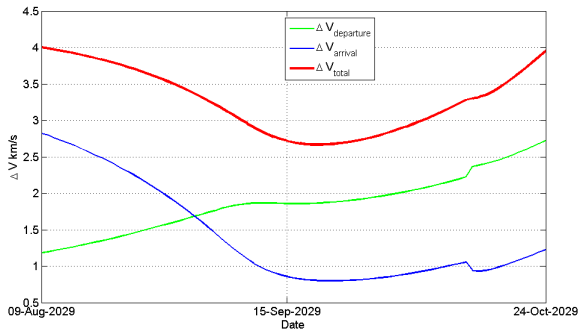

Figure 14: Launch window 2.

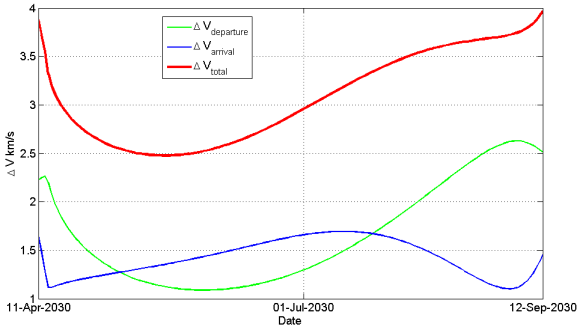

Figure 15: Launch window 3.

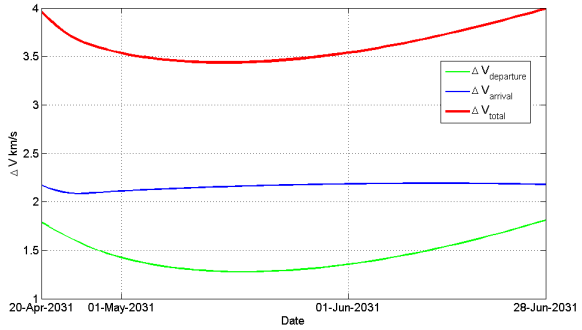

Figure 16: Launch window 4.

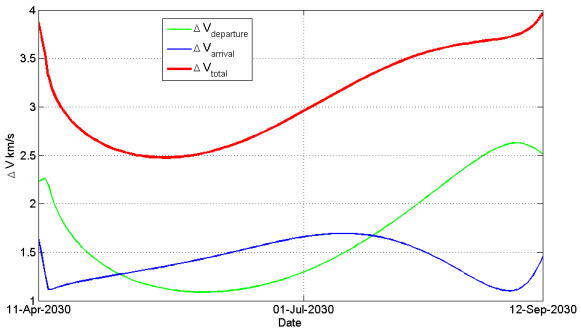

Figure 17: Launch window 5.

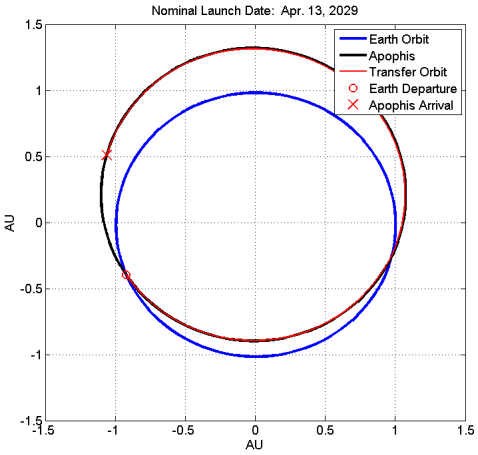

Figure 18: Nominal trajectory launch window 1. Trajectory shown in (X,Y) plane of J2000 coordinate system.

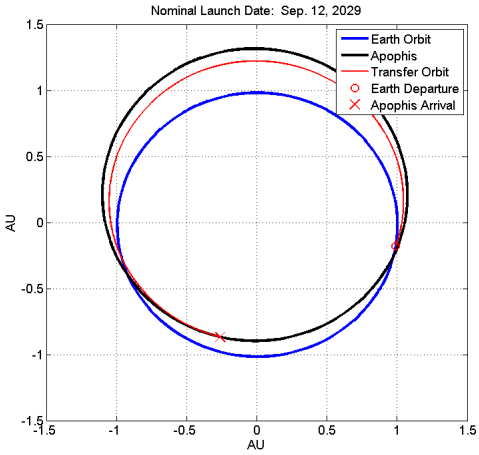

Figure 19: Nominal trajectory launch window 2. Trajectory shown in (X,Y) plane of J2000 coordinate system.

1-Revolution Nonimal Trajectories

Low Energy Rendezvous Mission Plots

The plots for the high energy solutions will not be shown in this appendix. In general the trajectory plots are very similar to the low energy solutions shown above.

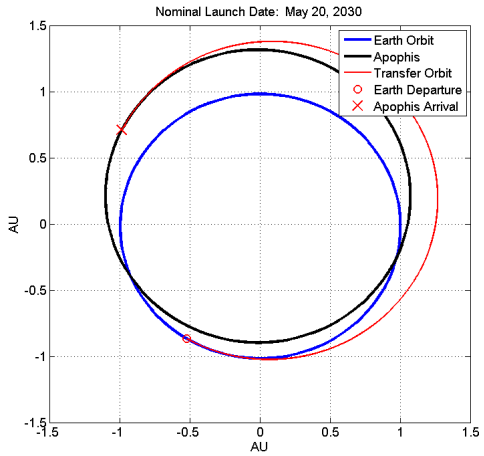

Figure 20: Nominal trajectory launch window 3. Trajectory shown in (X,Y) plane of J2000 coordinate system.

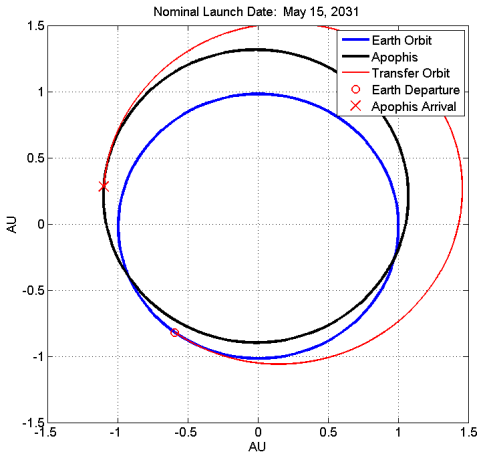

Figure 21: Nominal trajectory launch window 4. Trajectory shown in (X,Y) plane of J2000 coordinate system.

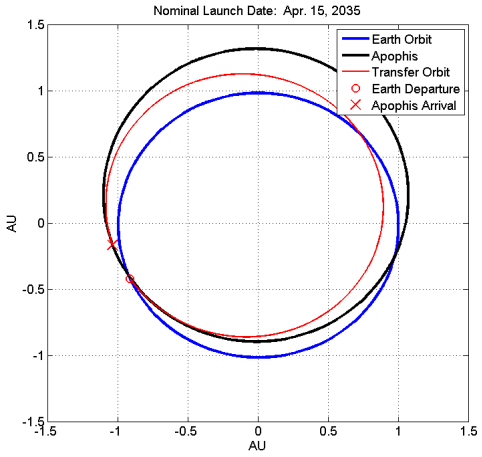

Figure 22: Nominal trajectory launch window 5. Trajectory shown in (X,Y) plane of J2000 coordinate system.

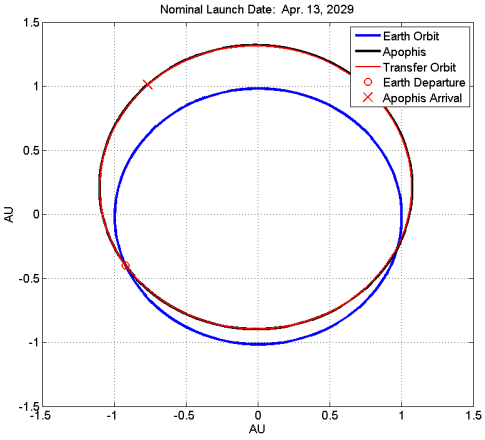

Figure 23: Nominal trajectory launch window 1 for the low energy 1 revolution solution. Trajectory shown in (X,Y) plane of J2000 coordinate system.

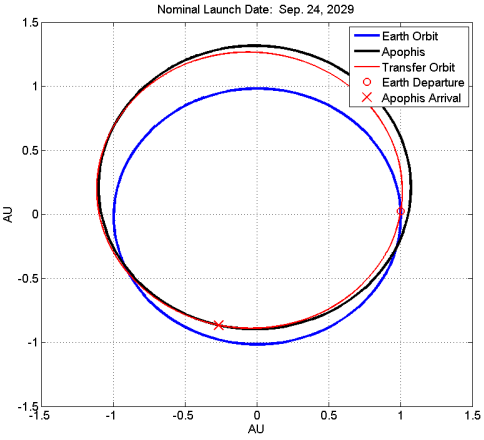

Figure 24: Nominal trajectory launch window 2 for the low energy 1 revolution solution. Trajectory shown in (X,Y) plane of J2000 coordinate system.

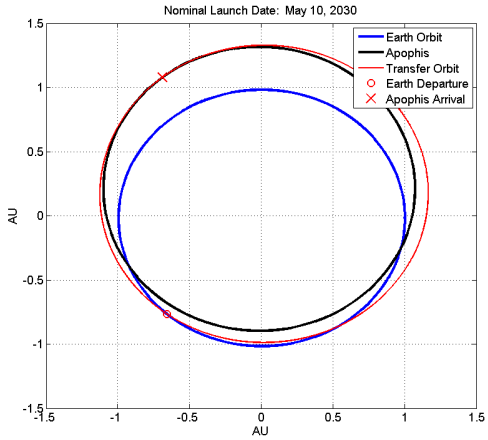

Figure 25: Nominal trajectory launch window 3 for the low energy 1 revolution solution. Trajectory shown in (X,Y) plane of J2000 coordinate system.

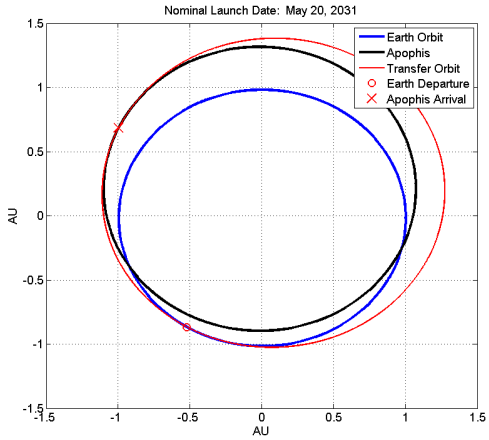

Figure 26: Nominal trajectory launch window 4 for the low energy 1 revolution solution. Trajectory shown in (X,Y) plane of J2000 coordinate system.

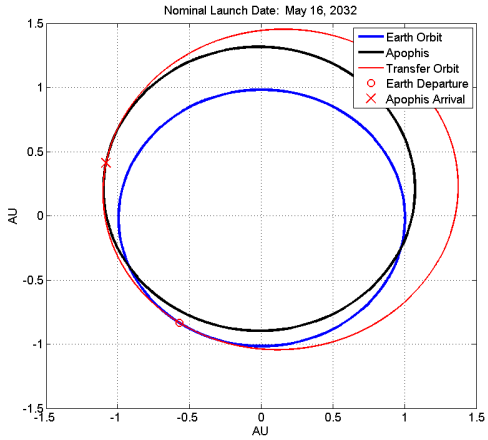

Figure 27: Nominal trajectory launch window 5 for the low energy 1 revolution solution. Trajectory shown in (X,Y) plane of J2000 coordinate system.

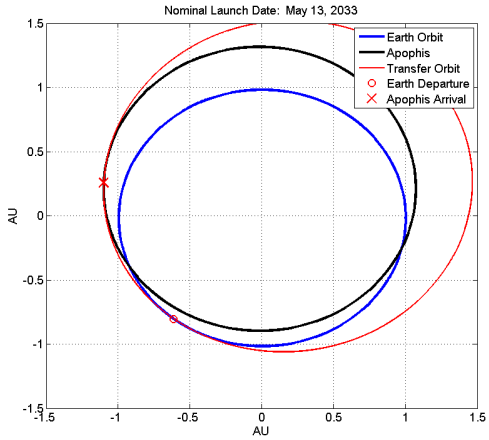

Figure 28: Nominal trajectory launch window 6 for the low energy 1 revolution solution. Trajectory shown in (X,Y) plane of J2000 coordinate system.

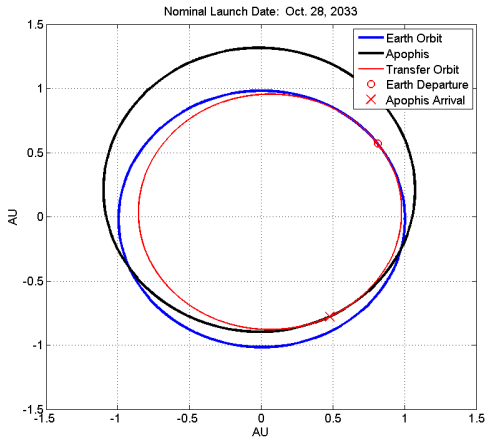

Figure 29: Nominal trajectory launch window 7 for the low energy 1 revolution solution. Trajectory shown in (X,Y) plane of J2000 coordinate system.

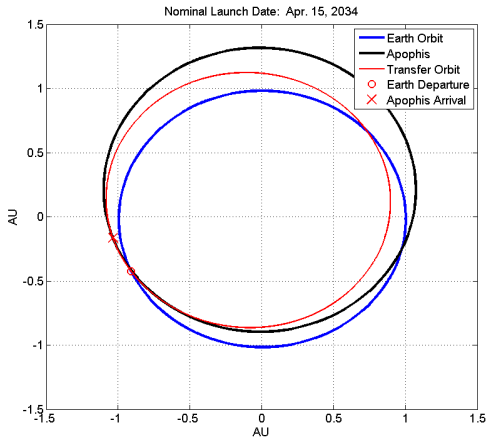

Figure 30: Nominal trajectory launch window 8 for the low energy 1 revolution solution. Trajectory shown in (X,Y) plane of J2000 coordinate system.

Appendix B: Solution to Lambert's Problem

The purpose of this appendix is to lay the ground work necessary to build a computational tool for obtaining the trajectories and results presented in this paper. Several solutions to Lambert's problem have been tested to determine the most efficient solution. Ephemeris data will be needed to calculate the positions of the Earth and each asteroid that is tested.

For any given two position vectors and the time-of-flight (TOF), the orbit determination problem is called Lambert's problem. For this reason Lambert's problem is well suited for an initial orbit determination and searching technique. In Lambert's problem the two position vectors and the TOF are known, but the orbit connecting those two points is unknown. The classical Kepler problem is used to determine a position as a function of time where the initial position and velocity vectors are known. Various solutions so Lambert's problem can be found in the literature.[12–15] While many solutions methods have been proposed, three commonly used methods are the classical universal variable method,[12,13,15] Battin's more recent approach using an alternate geometric transformation than Gauss' original method,[14,15] and the method developed by Lancaster and Blanchard[9] with improvement and additional details provided by R.H. Gooding.[7,8] The search for launch dates often requires Lambert's problem to be solved thousands, often millions of time. For this reason the object of this section is to outline the most efficient method to solve Lambert's problem.

A. Lambert Problem Definition

In Lambert's problem the initial and final radius vectors and time-of-flight are given respectively as, $\vec{r}_0$, $\vec{r}$, and Δt. The magnitudes of $\vec{r}_0$ and $\vec{r}$ are defined as r_0 and r. The following parameters are also needed for the post processing for each solution method.

$$c = \mid \vec{r} - \vec{r}_0 \mid \tag{1}$$

$$s = \frac{r_0 + r + c}{2} \tag{2}$$

A method to determine the transfer angle $\Delta\theta$ without quadrant ambiguity is described below.[13] The transfer angle $\Delta\theta$ for a prograde orbit is determined as follows:

$$\Delta\theta = \begin{cases} \cos^{-1}\left(\dfrac{\vec{r}_0 \cdot \vec{r}}{r r_0}\right) & \text{if } (\vec{r}_0 \times \vec{r}) \geq 0 \\ 360^o - \cos^{-1}\left(\dfrac{\vec{r}_0 \cdot \vec{r}}{r r_0}\right) & \text{if } (\vec{r}_0 \times \vec{r}) < 0 \end{cases} \tag{3}$$

Similarly the transfer angle for a retrograde orbit is determined as:

$$\Delta\theta = \begin{cases} \cos^{-1}\left(\dfrac{\vec{r}_0 \cdot \vec{r}}{r r_0}\right) & \text{if } (\vec{r}_0 \times \vec{r}) < 0 \\ 360^o - \cos^{-1}\left(\dfrac{\vec{r}_0 \cdot \vec{r}}{r r_0}\right) & \text{if } (\vec{r}_0 \times \vec{r}) \geq 0 \end{cases} \tag{4}$$

B. Battin's Solution

Let's consider Battin's approach first proposed in the 1980's and later published in his book.[14] This solution is similar to the method used by Gauss, but moves the singularity from 180◦ to 360◦ and dramatically improves convergence when the θ is large. It should also be noticed that Battin's solution works for all types of orbits (elliptical, parabolic, and hyperbolic) just as Gauss's original solution does. Throughout this section a brief outline of Battin's solution will be given. Any details left out can be found in Battin's book.[14]

1. Geometric Transformation of Orbit

Lambert's problem states that the time-of-flight is a function of a, $r_0 + r$, and c. Therefore the orbit can be transformed to any shape desired as long as the semi-major axis a, $r_0 + r$, and c are held constant. For Battin's formulation[10,14,16] the orbit is transformed such that the semi-major axis is perpendicular to the line from $\vec{r}_0$ to $\vec{r}$, which is c by definition.

The geometry of the transformed ellipse is shown in Battin's book.[14] From here the equation for the pericenter radius, r_p, is given below. The details leading up to this function can be found in Ref. [14].

$$r_p = a(1-e_0) = r_{0p}\sec^2\frac{1}{4}(E-E_0) \tag{5}$$

where e_0 is the eccentricity of the transformed orbit, while r_{0p} is the mean point of the parabolic orbit.[14] The mean point of the parabolic radius r_{0p} is also given by:[14]

$$r_{0p} = \sqrt{r_0 r}\left[\cos^2\left(\frac{\Delta\theta}{4}\right) + \tan^2(2w)\right] \tag{6}$$

The value of $\tan^2(2w)$ is needed for the calculation, which will be defined later. Next Kepler's time of flight equation can be transformed into a cubic equation, which must then be solved. First y will be defined as:

$$y^2 \equiv \frac{m}{(\ell+x)(1+x)} \tag{7}$$

Kepler's time-of-flight equation can now be represented by the following cubic equation.

$$y^3 - y^2 - \frac{m}{2x}\left(\frac{\tan^{-1}\sqrt{x}}{\sqrt{x}} - \frac{1}{1+x}\right) = 0 \tag{8}$$

In the above equation l, m, and x are always positive and are defined below. To calculate l, the following two equations, dependent only on the geometry of the problem, are also necessary.

$$\epsilon = \frac{r-r_0}{r_0} \tag{9}$$

$$\tan^2(2w) = \frac{\dfrac{\epsilon^2}{4}}{\sqrt{\dfrac{r}{r_0}} + \dfrac{r}{r_0}\left(2+\sqrt{\dfrac{r}{r_0}}\right)} \tag{10}$$

Using Eqs. (9) and (10), ℓ can be calculated as follows.

$$\ell = \frac{\sin^2\left(\dfrac{\Delta\theta}{4}\right) + \tan^2(2w)}{\sin^2\left(\dfrac{\Delta\theta}{4}\right) + \tan^2(2w) + \cos\left(\dfrac{\Delta\theta}{2}\right)} \qquad 0^o < \Delta\theta \leq 180^o \tag{11}$$

$$\ell = \frac{\cos^2\left(\dfrac{\Delta\theta}{4}\right) + \tan^2(2w) - \cos\left(\dfrac{\Delta\theta}{2}\right)}{\cos^2\left(\dfrac{\Delta\theta}{4}\right) + \tan^2(2w)} \qquad 180^o < \Delta \leq < 360^o \tag{12}$$

$$m = \frac{\mu\Delta t^2}{8r_{op}^3} \tag{13}$$

$$x = \sqrt{\left(\frac{1-\ell}{2}\right)^2 + \frac{m}{y^2}} - \frac{1+\ell}{2} \tag{14}$$

Initial conditions for x that guarantee convergence are:

$$x_0 = \begin{cases} 0 & \text{parabola, hyperbola} \\ \ell & \text{ellipse} \end{cases} \tag{15}$$

The cubic function (Eq. (8)) can now be solved using the following sequential substitution method:

1. An initial estimation of x is given by Eq. (15).
2. Calculate all the values needed for the cubic from Eqs. (9), (10), (11) or (12), and (13).

3. Solve the cubic Eq. (8) for y.

4. Use Eq. (14) to determine a new value for x.

5. Repeat the above 3 steps until x stops changing.

We now have a nearly complete solution algorithm for Lambert's problem, although solving the cubic function is not a trivial matter. Battin[14] next develops a method to flatten the cubic function to improve the convergence rate, as well as a method using continued fractions to determine the largest real positive root of the cubic function. The following section gives the equations necessary to find the flattening parameters and solve the cubic function.

2. *Use of Free Parameter to Flatten Cubic Function*

The cubic equation, Eq. (8), from the previous section can now be represented in terms of the flattening parameter functions, h_1 and h_2, as follows:

$$y^3 - (1 + h_1)y^2 - h_2 = 0 \tag{16}$$

The flattening parameters can be represented in terms of x, l, and m as

$$h_1 = \frac{(l + x)^2(1 + 3x + \xi)}{(1 + 2x + l)[4x + \xi(3 + x)]} \tag{17}$$

$$h_2 = \frac{m(x - l + \xi)}{(1 + 2x + l)[4x + \xi(3 + x)]} \tag{18}$$

The function $\xi(x)$ needed for the calculation of h_1 and h_2 is calculated from the continued fraction as follows:

$$\xi(x) = \cfrac{8(\sqrt{1+x}+1)}{3 + \cfrac{1}{5 + \eta + \cfrac{\frac{9}{7}\eta}{1 + \cfrac{\frac{16}{63}\eta}{1 + \cfrac{\frac{25}{99}\eta}{1 + \cfrac{\frac{36}{143}\eta}{1 + \ddots}}}}}}} \tag{19}$$

where η is defined as

$$\eta = \frac{x}{(\sqrt{1+x}+1)^2} \qquad \text{where} \qquad -1 < \eta < 1 \tag{20}$$

3. *Solving the Cubic Function*

In this section a method to determine the largest real root of Eq. (16) is outlined. Using this method a successive algorithm can be used ultimately to determine the f and g functions, given by Ref. [12,15]. Using the Lagrangian f and g functions the initial and final velocity vectors are then obtained. The first step is to calculate B and u as follows:

$$B = \frac{27h_2}{4(1 + h_1)^3} \tag{21}$$

$$u = \frac{B}{2(\sqrt{1+B}+1)} \tag{22}$$

Also, $K(u)$ is the calculated from the continued fraction

$$K(u) = \cfrac{\frac{1}{3}}{1 + \cfrac{\frac{4}{27}u}{1 + \cfrac{\frac{8}{27}u}{1 + \cfrac{\frac{2}{9}u}{1 + \cfrac{\frac{22}{81}u}{1 + \ddots}}}}} \tag{23}$$

where the coefficients for the odd and even coefficients of u are generally obtained from the following two equations.

$$\gamma_{2n+1} = \frac{2(3n+2)(6n+1)}{9(4n+1)(4n+3)} \tag{24}$$

$$\gamma_{2n} = \frac{2(3n+1)(6n-1)}{9(4n-1)(4n+1)} \tag{25}$$

The largest positive real root for the cubic equation is calculated as

$$y = \frac{1+h_1}{3}\left(2 + \frac{\sqrt{1+B}}{1+2u(K^2(u))}\right) \tag{26}$$

The cubic function (Eq. (16)) can now be solved using the following sequential substitution method.

1. An initial estimation of x is given by Eq. (15).
2. Calculate all the values needed for the flattening parameters Eqs.(17) and (18) from Eqs. (9), (10), (11) or (12), and (13).
3. Calculate $\eta(x)$ from Eqs. (19) and (20).
4. Calculate $K(u)$ using Eqs. (21), (22), and (23)
5. Calculate the solution for the cubic function using Eq. (26) for y.
6. Use Eq. (14) to determine a new value for x.
7. Repeat the above 5 steps until x stops changing.

The next step is to determine the semi-major axis of the orbit. If the semi-major axis is positive,the orbit is elliptical, and the initial and final velocity vectors can be calculated as follows. The hyperbolic and parabolic velocity vectors are calculated in a similar manner.[15]

$$a = \frac{\mu(\Delta t)^2}{16 r_{op}^2 x y^2} \tag{27}$$

4. Determining the Lagrange Coefficients for Elliptical Orbits

The Lagrange coefficients for the elliptical orbit case can be calculated from the following set of equations.

$$\beta_e = 2\sin^{-1}\sqrt{\frac{s-c}{2a}} \tag{28}$$

$$\beta_e = -\beta_e \quad \text{If } \Delta\theta > \pi \tag{29}$$

$$a_{min} = \frac{s}{2} \tag{30}$$

$$t_{min} = \sqrt{\frac{a_{min}^3}{\mu}}(\pi - \beta_e + \sin\beta_e) \tag{31}$$

$$\alpha_e = 2\sin^{-1}\sqrt{\frac{s}{2a}} \tag{32}$$

$$\alpha_e = 2\pi - \alpha_e \quad \text{If } \Delta t > t_{min} \tag{33}$$

$$\Delta E = \alpha_e - \beta_e \tag{34}$$

The Lagrangian coefficients can be calculated as follows:

$$f = 1 - \frac{a}{r_0}(1 - \cos\Delta E) \tag{35}$$

$$g = \Delta t - \sqrt{\frac{a^3}{\mu}}(\Delta E - \sin\Delta E) \tag{36}$$

$$\dot{g} = 1 - \frac{a}{r}(1 - \cos\Delta E) \tag{37}$$

With the Lagrangian coefficients now known, the initial and final velocity vectors can be found from the following equations.

$$\vec{v}_0 = \frac{\vec{r} - f\vec{r}_o}{g} \tag{38}$$

$$\vec{v} = \frac{\dot{r}\vec{r} - \vec{r}_o}{g} \tag{39}$$

This concludes the solutions to Lambert's problem using Battin's method.

C. Bate, Mueller and White Universal Method

In this section one of the methods used for the multiple revolution Lambert solutions will be presented. This solution is a universal method first proposed by Bate, Mueller, and White[12] and covered extensively in literature.[11,13,15] Another method, which uses Gooding's[7,8] extension to the universal method formulated by Lancaster,[9] was used to confirm the result from the BMW method.

In this method the time-of-flight equation can be written as:

$$\sqrt{\mu}t = x^3 S + A\sqrt{y} \tag{40}$$

Where S and C are the Stumpff functions[12] and x, y, and A are:

$$x = \sqrt{\frac{y}{C}} \tag{41}$$

$$y = r_0 + r - \frac{A(1 - zS)}{\sqrt{C}} \tag{42}$$

$$A = \frac{\sqrt{r_0 r}\sin\theta}{\sqrt{1 - \cos\theta}} = \pm\sqrt{r_0 r(1 + \cos\theta)} \tag{43}$$

Where + for a prograde orbit and - for a retrograde orbit.

A plot of the universal time-of-flight equation 40 is shown in Fig. 31. The 0-revolution solutions are found in the region up to $4\pi^2$, with the multiple revolution region occuring when z is greater than $4\pi^2$. The regions are bounded by:

$$4n^2\pi^2 < z < 4(n+1)^2\pi^2 \tag{44}$$

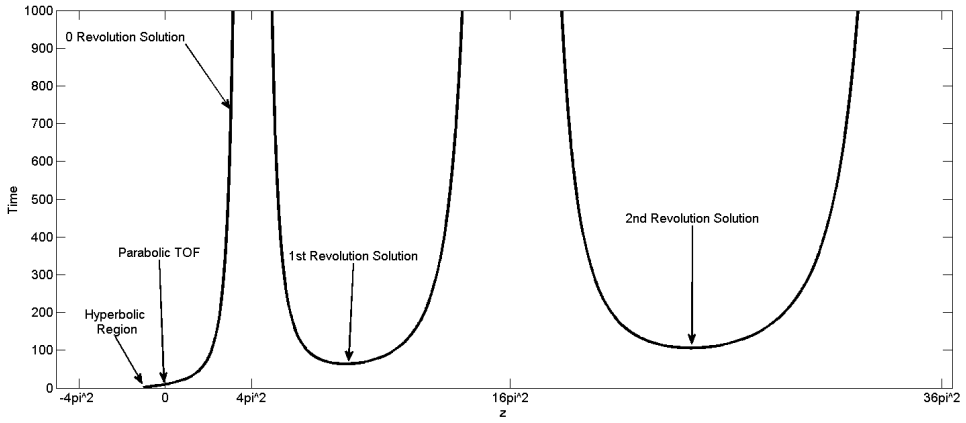

Figure 31: Universal time-of-flight function showing various solution regions.

The number of complete revolutions is represented by n.

As Figure 31 indicates there are two solutions for each N-revolution orbits. The left branch is the long-period solution, referred to in this paper as the high-energy solution, with the right branch being the short-period solution, referred to as the low-energy solution. The minimum time-of-flight for a N-revolution orbit can be found by solving the derivative of the time-of-flight equation. The two solution branches can then be solved by root solving the time-of-flight equation. More information on this solution method can be found in BMW[12] and Arora and Russell.[11]

D. Computational Efficiency for 0-Revolution Solution Methods

In this section an overview of the performance obtained from various Lambert problem solutions will be discussed. The three methods covered in this section are Battin's solution (discussed above), a universal variable using a Newton method, similar to BMW[12] and Curtis,[13] and lastly a universal variable solution using the bisection method, similar to Vallado.[15]

Table 6: Information on the computer used for the computational efficiency study.

Model	Dell T3500 Workstation
Operating System	Windows Vista Enterprise 64 bit
Processor	2 x Intel(R) Xeon(R) W3520 2.67 GHz
Memory	6.00 GB 1066 Mhz DDR3
Matlab	R2009b-64 bit

For all calculations Matlab R2009b (64 bit version) was used. A compile environment would likely increase the general speed of the program, however the program is being written so the final version can be easily used and modified by others. Table 6 has all the information relevant to the computer used for these calculations. The computer used was a dual quad core Xeon processor (8 total cores) running Windows Vista Enterprise.

In each case the program was run for an example case that is representative of cases that the program would be likely to be used for. In this case it was ran to compute a porkchop plot for an asteroid rendezvous mission. A plot of the number of solutions per second for each of the three solutions is given in Figure 32. Analysis of this plot indicates that the Battin solution is significantly more efficient than either the Newton or bisection solutions. In the same way the Newton universal variable solution is much slower than the bisection method. In general the Newton method would be expected to be more efficient than a bisection method. In this case it is likely that the Newton method doesn't always converge and runs through every loop iteration allowed by the program. On average the Battin solution is 8.94 times faster than the bisection method and 158.66 times faster than the Newton solution method. The maximum number of solutions obtain using all 8 cores (maximum in every case) for the Battin, Newton, and bisection method are 14317, 1867, and 174 respectively.

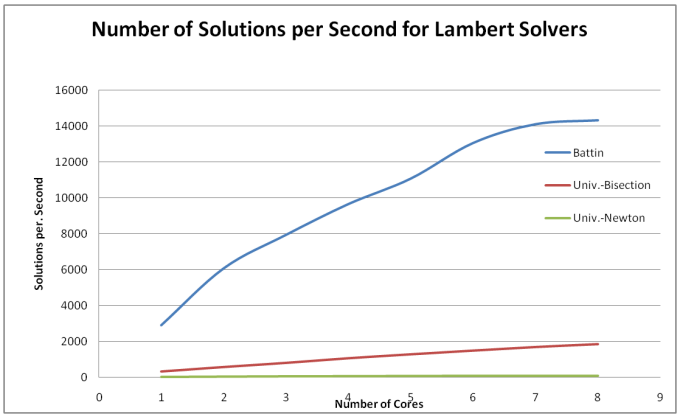

Figure 32: Plot of number of solutions per second versus number of cores for various Lambert solution methods.

IV. Acknowledgments

This work was supported by the Iowa Space Grant Consortium (ISGC) through a research grant to the Asteroid Deflection Research Center at Iowa State University. The authors would like to thank Dr. William Byrd (former Director, ISGC) for his interest and support of this research work.

References

[1]Wie, B., *Space Vehicle Dynamics and Control*, American Institute of Aeronatics and Astronautics, Inc., Reston, VA 20191, 2nd ed., 2008.

[2]Wie, B. and Dearborn, D., "Earth-Impact Modeling and Analysis of a Near-Earth Object Fragmented and Dispersed by Nuclear Subsurface Explosions," *20th AAS/AIAA Space Flight Mechanics Meeting*, , No. AAS 10-137, Feb. 2010.

[3]Wie, B., "Dynamics and Control of Gravity Tractor Spacecraft for Asteroid Deflection," *Journal of Guidance, Control, and Dynamics*, Vol. 31, No. 5, Nov. 2008, pp. 1413–1423.

[4]Wagner, S., Pitz, A., Zimmerman, D., and Wie, B., "Interplanetary Ballistic Missile (IPBM) System Architecture Design for Near-Earth Object Threat Mitigation," *60th International Astronautical Congress*, Vol. IAC-09, No. D1.1.1, Oct. 2009.

[5]Wagner, S. and Wie, B., "Minimum ΔV Launch Windows for a Fictive Post-2029 Apophis Deflection/Disruption Mission," *AAS*, Vol. 10, No. 245, Feb. 2010.

[6]SpaceWorks-Engineering-Inc and SpaceDev-Inc., "Foresight: A Radio Tagging Mission to Near Earth Asteroid Apophis," *Planetary Society 2007 Apophis Mission Design Competition*, Aug. 2007.

[7]Gooding, R., "On the Solution of Lambert's Orbital Boundary-Value Problem," *Royal Aerospace Establishment*, Apr. 1988.

[8]Gooding, R., "A Procedure for the Solution of Lambert's Orbital Boundary-Value Problem," *Kluwer Academic Publishers*, Jan. 1990.

[9]Lancaster, E. and Blanchard, R., "A Unified Form of Lambert's Theorem," *NASA Technical Note*, Sept. 1969.

[10]Shen, H. and Tsiotras, P., "Using Battin's Method to Obtain Multiple-Revolution Lambert's Solutions," *American Astronautical Society*, Vol. 116, 2003.

[11]Arora, N. and Russell, R., "GPU Accelerated Multiple Revolution Lambert Solver for Fast Mission Design," *AAS*, Vol. 10.

[12]Bate, R., Mueller, D., and White, J., *Fundamentals of Astrodynamics*, Dover Publications, Inc., 180 Varick Street, New York, NY, 1st ed., 1971.

[13]Curtis, H., *Orbital Mechanics for Engineering Students*, Elsevier Butterworth-Heinemann, Linacre House, Jordan Hill, Oxford, 1st ed., 2005.

[14]Battin, R., *An Introduction to the Mathematics and Methods of Astrodynamics, Revised Edition*, AIAA Educational Series, 1801 Alexadner Bell Drive, Reston, VA, revised edition ed., 1999.

[15]Vallado, D., *Fundamentals of Astrodynamics and Applications*, Microcosm Press, 401 Coral Circle, El Segundo, CA, 2nd ed., 2004.

[16]Loechler, L., *An Elegant Lambert Algorithm for Multiple Revolution Orbits*, Master's thesis, Massachusetts Institute of Technology, May 1988.